

Research Article

Efficient surface enhanced Raman scattering substrates based on complex gold nanostructures formed by annealing sputtered gold thin films

Thi Huyen Trang Nguyen^a, Thi Mai Anh Nguyen^b, Cong Doanh Sai^a, Thi Hai Yen Le^a,
Thi Ngoc Anh Tran^a, Thanh Cong Bach^a, Van Vu Le^a, Nguyen Hai Pham^a, An Bang Ngac^a, Viet
Tuyen Nguyen^{a,*}, Thi Ha Tran^{a,c,**}

^a Faculty of Physics, University of Science, Vietnam National University, Hanoi, 334 Nguyen Trai, Thanh Xuan, Hanoi, Viet Nam

^b HUS High School for Gifted Students, 182 Luong The Vinh, Thanh Xuan, Hanoi, Viet Nam

^c Faculty of Fundamental Sciences, Hanoi University of Mining and Geology, Duc Thang, Tu Liem, Hanoi, Viet Nam



ARTICLE INFO

Keywords:

Gold nanoparticles
Sputtering
Annealing
Plasmon
Surface enhanced Raman scattering

ABSTRACT

Surface enhanced Raman scattering (SERS) has attracted great attention of scientists in the last few decades due to its wide range of applications, especially in detecting chemical compounds even at single molecular level. In this research, we combine sputtering and post annealing method to prepare gold nanoparticles with uniform distribution on cover glass substrates, which work as efficient SERS substrates. This work studies the effect of gold thickness on the formation of nanoparticles during annealing process. The effect of size, inter-distance and morphology of gold NPs on plasmon properties was studied by scanning electron microscope and absorption spectroscopy. The enhancement capability of different morphologies was also verified by using Finite Different Time Domain (FDTD) technique. The as-prepared gold nanoparticles arrays are efficient surface enhanced Raman scattering substrates as demonstrated by the ability to detect methylene blue at concentration as low as 10^{-10} M. The facile, cost-effective fabrication process is convenient to scale up for mass production of high sensitivity surface enhanced Raman substrates.

1. Introduction

Raman spectroscopy is an optical technique that analyzes inelastic scattering light from materials. Thanks to the unique vibrational modes of characterized chemical bonds in molecules, Raman spectra can provide “fingerprint-signal” for identification of substances. Low probability of Raman scattering of only about 10^{-6} prevents realizing practical applications. Since its discovery, surface-enhanced Raman scattering (SERS) is expected to provide a great tool to detect substances at very low concentration, which is necessary for applications in various fields such as chemical sensing, biology and medicine [1–4].

Typical SERS substrates are roughened thin films or self-assembled arrays of noble metal nanoparticles (NPs). If the inter-distances between these NPs are in the nanometer scale, the strong interaction among particles leads to localized surface plasmon resonance (LSPR) [5, 6]. LSPR effect can amplify Raman signal of organic molecules by several orders of magnitude. Regarding enhancement of the

electromagnetic field by the excitation of LSPR, the gaps between metal NPs (or “nanogaps”) were believed to play a vital role [5,6]. SERS substrates based on gold or silver nanoparticles were studied by many groups using solution methods [7–12]. Self-assembled monolayers of NPs developed from solution phase were reported to be good SERS substrates of low cost and high enhancement ability. However, the main limitations of these substrates are the high randomness of NPs distribution during the synthetic process, difficulties in controlling particle size and shapes. As hot-spots are mostly generated in the inter-particle region, the uniform distribution of nanoparticles affects significantly the distribution of “hot-spot” regions, which in turn, is crucial to the repeatability of SERS substrates [5,6,13]. The high deviation of SERS signal is an obstacle to quantitative analysis based on SERS.

Furthermore, surfactants, usually utilized in chemical approach, might limit the chemical activity of nanoparticles and/or interfere to the signals of Raman probe. In this paper, we report the results of growth of gold nanoparticles arrays on cover glass by a facile, pure physical

* Corresponding author.

** Corresponding author. Hanoi University of Mining and Geology, 18 Vien Street, Duc Thang, North Tu Liem, Hanoi, Vietnam.

E-mail addresses: nguyenvietuyen@hus.edu.vn (V.T. Nguyen), tranthiha@hmg.edu.vn (T.H. Tran).

approach combining sputtering and thermal annealing processes. Effect of sputtering time on morphology, surface plasmon resonance and Raman enhancement capability of gold nanoparticles were studied in details. The experimental data was also supported with simulation by Finite Different Time Domain (FDTD) technique.

2. Experiment

2.1. Fabrication of Au- nanostructures on glass substrates

Cover glasses with the dimension of 22×22 mm, purchased from Merck (Germany), were cleaned by ultrasonic bath in acetone, ethanol and double distilled water sequentially in 2 min for each cycle. The glass substrates were then dried by nitrogen blowing. A DC sputtering system (JEOL JFC – 1200) was used to sputter gold films on the cleaned glass substrates. A pure gold target in form of a round disk with diameter of 2 inches and thickness of 3 mm was used as supplied by Matsurf Technologies Inc, USA, without further purification. Sputtering current was kept constant at 20 mA while different sputtering time from 10 to 70 s (with a step of 10 s) was applied to prepare gold thin films of different thicknesses. The thickness of gold films on glass substrates was estimated by using the calibration data for gold target provided by the sputtering system providers. The thickness was also further verified by using crystal quark vibration method available in the system. The thickness of films increases from 2 nm to 10 nm, correspondingly when the sputtering time increases from 10 s to 70 s. The obtained thin films were then annealed in a furnace at 300°C in 2 h in ambient condition to form nanoparticle array.

2.2. Sample characterization: SEM, UV-Vis and Raman spectroscopy

A field emission scanning electron microscope Nova Nano SEM FEI 450 was used to investigate the morphologies of samples. The surface plasmon resonance properties of the as-synthesized nanostructures on glass substrates were analyzed via absorption spectra collected on UV-Vis Jasco V – 750 spectrometer. Prior to absorption measurement, a baseline process was performed on bare substrate to guarantee that the absorption of glass substrates was excluded and only absorption of gold thin films was collected.

For Raman measurements, methylene blue (MB), received from Sigma Aldrid, was used as a Raman probe. $10 \mu\text{l}$ of MB solutions of different concentrations (10^{-7} M, 10^{-8} M, 10^{-9} M, 10^{-10} M) were absorbed on the surface of samples and naturally dried. Labram 800 from Horiba with excitation wavelength of 632.8 nm was utilized to collect Raman spectra. Laser power at the surface sample was fixed at 0.5 mW for all measurement to minimize any heat effect interference.

3. Results and discussion

Morphology of the prepared samples was observed by Scanning Electron Microscope. Fig. 1 presents SEM images of gold arrays prepared with sputtering time of 10, 20, 30, 40, 50, 60 and 70 s with heat treatment at 300°C in 2 h. Sputtering time of 10 s is expected to the deposition a 2 nm thick gold film. After being heated, gold layer was transformed into nanoparticles with spherical shape. As the sputtering time rose, corresponding to the increase of Au thickness, the size of particles dramatically increased and thus, affected directly to the distribution of particles on substrates. However, it is likely that the film deposited in 70 s was so thick that shrinkage of gold layer could not occur to form particle structure after heating process.

Sputtering of less than 40 s offered products mainly of nanoparticles. Size distribution of gold nanoparticles was estimated from SEM images by using Image J software. Sputtering time of greater than 40 s leads to formation of complex structures of irregular shapes, hence size distribution is not available. It is obvious that sputtering time of 10 s offers particles of smallest size. The particles are uniformly distributed on

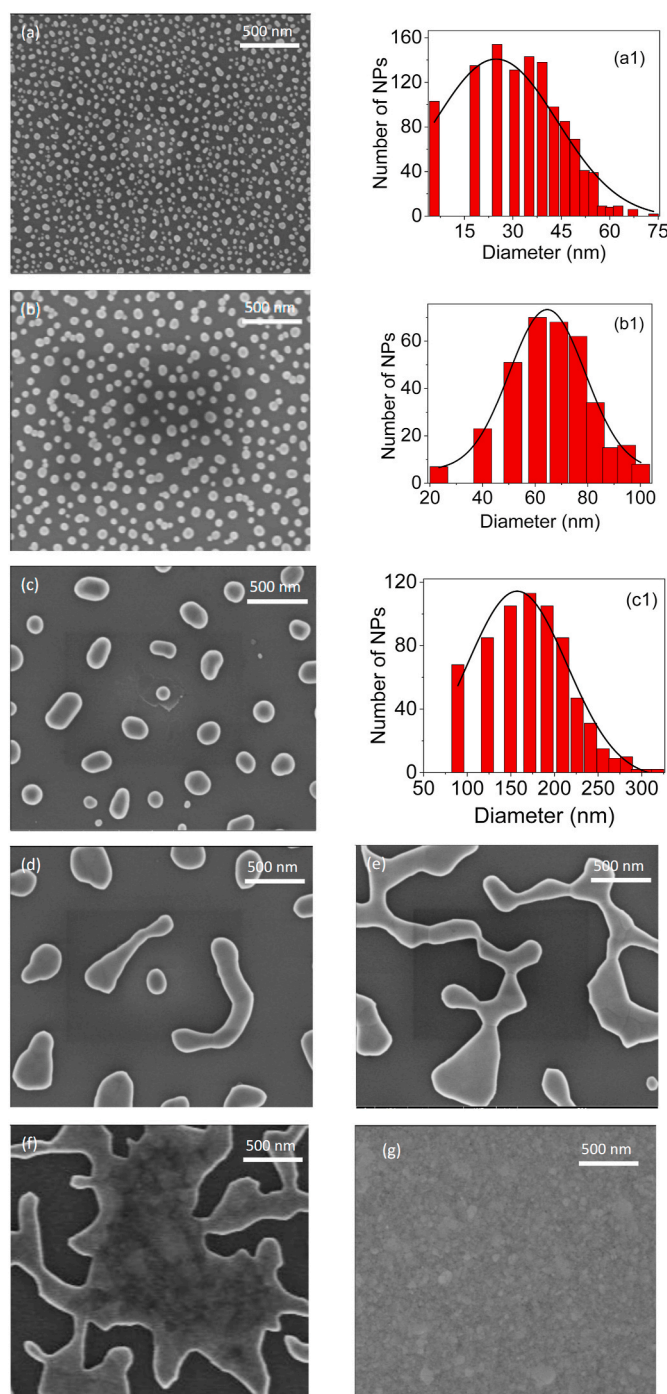


Fig. 1. SEM images of Au nanostructures obtained after heating gold thin films prepared with different sputtering time: (a) 10 s; (b) 20 s; (c) 30 s; (d) 40 s; (e) 50 s; (f) 60 s; (g) 70 s and the corresponding size distribution of samples prepared with sputtering time of: (a1) 10 s; (b1) 20 s; (c1) 30 s.

substrate at high density. The diameter of most particles is in the range from 20 nm to 50 nm, with the average distance of 25 nm. The average particle size grew rapidly to 60 and 150 nm and the inter-particle distances increased from 53 nm to 86 nm as the sputtering times increased to 20 and 30 s, respectively. Besides, SEM image (Fig. 1d) also showed that with sputtering time of 40 s, some complex structures rather than separated particles were formed. These structures became bigger and more dominant when further increasing sputtering times. As can be seen from Fig. 1f, heat treatment was barely enough to shrink the films into islands. Films prepared with sputtering time of longer than 70 s was too

thick to be converted into nanostructures by heating at 300 °C. Continuous film remained after heat treatment as presented in Fig. 1g.

Energy dispersive spectroscopy was used to verify the composition of the nanostructures. Typical spectra for samples prepared with sputtering time of 30 s and 40 s with and without annealing process are shown in Fig. 2. As can be seen from Fig. 2, only signals of Si and Au can be detected. Because Si peak belongs to the substrates, the data suggests that the samples were pure and clean. To further confirm the nature of the produced nano clusters, element mapping of the samples was studied. The mapping results by tracing the peak of gold at 2.14 keV are shown in Fig. 3. The good matching between the SEM images and distribution of gold element elucidates that the nanoclusters in the SEM images are gold.

LSPR of nanoparticles substantially depends on the size and shape of NPs as well as the distance between them [14]. Therefore, controlling morphology of NPs and their density is very important for enhancing Raman signal. According to theory, when the incident laser wavelength matches with the LSPR of metal NPs, the local electromagnetic field of NPs will be amplified greatly [15]. Fig. 4 shows the absorption spectra of all gold samples before and after heat treatment. The LSPR wavelengths of NPs were determined by the absorption peaks of spectra. It is obvious from Fig. 4a that no absorption peak was observed in spectra of all gold films without heat treatment. An absorption edge at 530 nm was observed for all thin films of gold. It is commonly accepted that this absorption edge relates to the bulk absorption modes of gold materials according to the dispersion equation for noble metal [16,17]. The appearance of this absorption edge implies that the obtained products are continuous flat films [18]. This explains for the independence of this peak position upon increasing sputtering time. The formation of gold NPs after heat treatment was reconfirmed by the appearance of clear LSPR absorption peaks as shown in Fig. 4b.

The absorption peak was found to redshift from 540 nm to 652 nm as sputtering time increases from 10 s to 40 s. The red-shift of absorbance peak show agreement with the fact that Au NPs gets bigger at longer sputtering time as shown by SEM images. At longer sputtering time, these peaks shift to over 700 nm. This huge peak shift likely relates to the formation of large Au structures instead of Au NPs [14,19]. Longer sputtering time not only changes peak position but also broaden the LSPR peaks. The change in absorption spectra is correlated to the distinct morphology and size of gold clusters in samples prepared with long sputtering time.

To maximize the strength of SERS signal, the LSPR wavelength of NPs should be close to the wavelength of the incident light. In this research, we used He Ne laser with wavelength of 632.8 nm to investigate SERS effects. For that reason, samples with coating times range

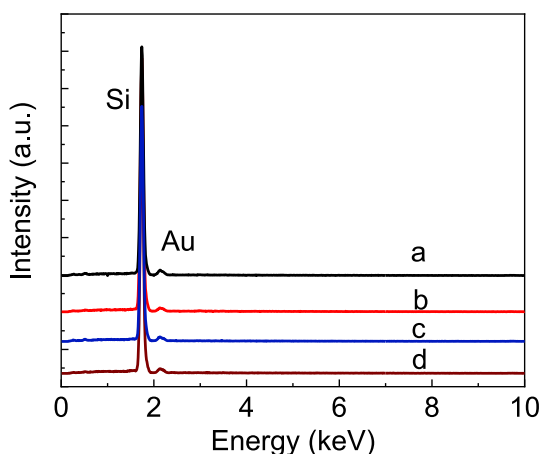


Fig. 2. Energy dispersive spectra of samples prepared with sputtering time of 30 s: a) before annealing; b) after annealing; and 40 s: c) before annealing; d) after annealing.

from 30 s to 50 s which have LSPR wavelengths at over 600 nm are expected to show the highest Raman signal. To demonstrate that Au NPs on cover glasses can work as effective SERS substrates, their surface enhanced Raman activities were studied with MB as a Raman probe.

First, MB at a low concentration of 10^{-7} M was used to investigate the Raman enhancement of the prepared SERS substrates. Fig. 5a shows Raman spectra of MB absorbed on gold nanoparticles samples prepared with different sputtering time (ranging from 10 s to 70 s). It is obvious that characterized peaks of MB can be detected clearly throughout the region from 600 to 1600 cm^{-1} . These peaks represent different type of vibrations in MB molecule structure, namely, the peak at 1622 cm^{-1} can be assigned to ring stretching of C–C while peak at 1298 cm^{-1} is due to the in-plane ring deformation of C–H. The symmetrical stretching mode of C–N can also be identified by 1390 cm^{-1} peak, and peak at 769 cm^{-1} was resulted from in-plane bending of C–H [15]. These characteristic peaks are observed in all spectra shown in Fig. 5a but the Raman intensities strongly depended on the sputtering time. The Raman data shows that the intensity increases significantly with increment of sputtering time from 10 s to 40 s. At sputtering time of 30 s and 40 s, the intensity of the two main peaks at 1622 cm^{-1} and 1390 cm^{-1} are highest when compared with those of other samples under same measurement condition. Further increasing sputtering time to over 50 s results in a dramatic drop of Raman signal.

To illustrate the dependence of Raman enhancement on sputtering time, the plot of intensity of the two main peaks at 1622 cm^{-1} and 1390 cm^{-1} vs. sputtering time was shown in Fig. 5b. As can be seen from Fig. 5b, the Raman intensities of these peaks are high when sputtering time is from 30 to 50 s. Especially, sputtering time from 30 s to 40 s shows the highest intensity of all characterized peaks. This result matches closely with expected results from absorption spectra.

According to the experimental results, two simulation processes were performed. Incident light was set at normal direction to the substrates. The first simulation model was processed for spherical gold nanoparticles with radius of 60 nm and inter-spacing of 20 nm. The second model represented the complex gold nanostructure obtained with sputtering time of 40 s and is conceptualized as a spherical nanoparticle of radius 100 nm locating at the center of a rod in the shape of a semi-circle of radius 150 nm. The simulation results are presented in Fig. 6. The simulation data suggests that hotspots formed between complex structures are also effective in enhancing Raman signal. It should be noted that the effective area in the second case is expanded much higher rather than only concentrates in the small nanogap between the two particles in the first case. From the experimental and theoretical data, it can be concluded that optimum sputtering time is between 30 s and 40 s and thus, these samples were further studied to determine their limit of detection. Fig. 7 shows Raman spectra of MB at different concentrations absorbed on Au nanoparticle array prepared with sputtering time of 30 and 40 s.

To investigate the limit of detection (LOD) of MB using the prepared SERS substrates, MB at different concentrations were absorbed on gold nanostructure arrays. As shown in Fig. 7, MB Raman signal declined monotonically as the concentration decreased. When the MB concentration decreased to 10^{-10} M, the characteristic peaks could still be observed. With the sample prepared with sputtering time of 30 s, Raman spectrum were multiplied 10 times for better visual when being shown with spectra of higher concentrations. It can be seen that Raman spectra of MB at low concentration could be detected more clearly with nanostructures obtained with sputtering time of 40 s. The results are in good agreement with the absorption spectra and simulation data. The LOD of 10^{-10} M achieved in this research is comparable with LODs of some other 2D SERS substrates in literature (Table 1) [20–26]. It should be noted that most of reported effective SERS substrates were prepared by multi-step processes, where advanced techniques, organic compounds or surfactants are required. Using of such compounds may degrade the surface properties of the noble metal nanostructures and in turn affects the enhancement capability of SERS substrates. In addition to

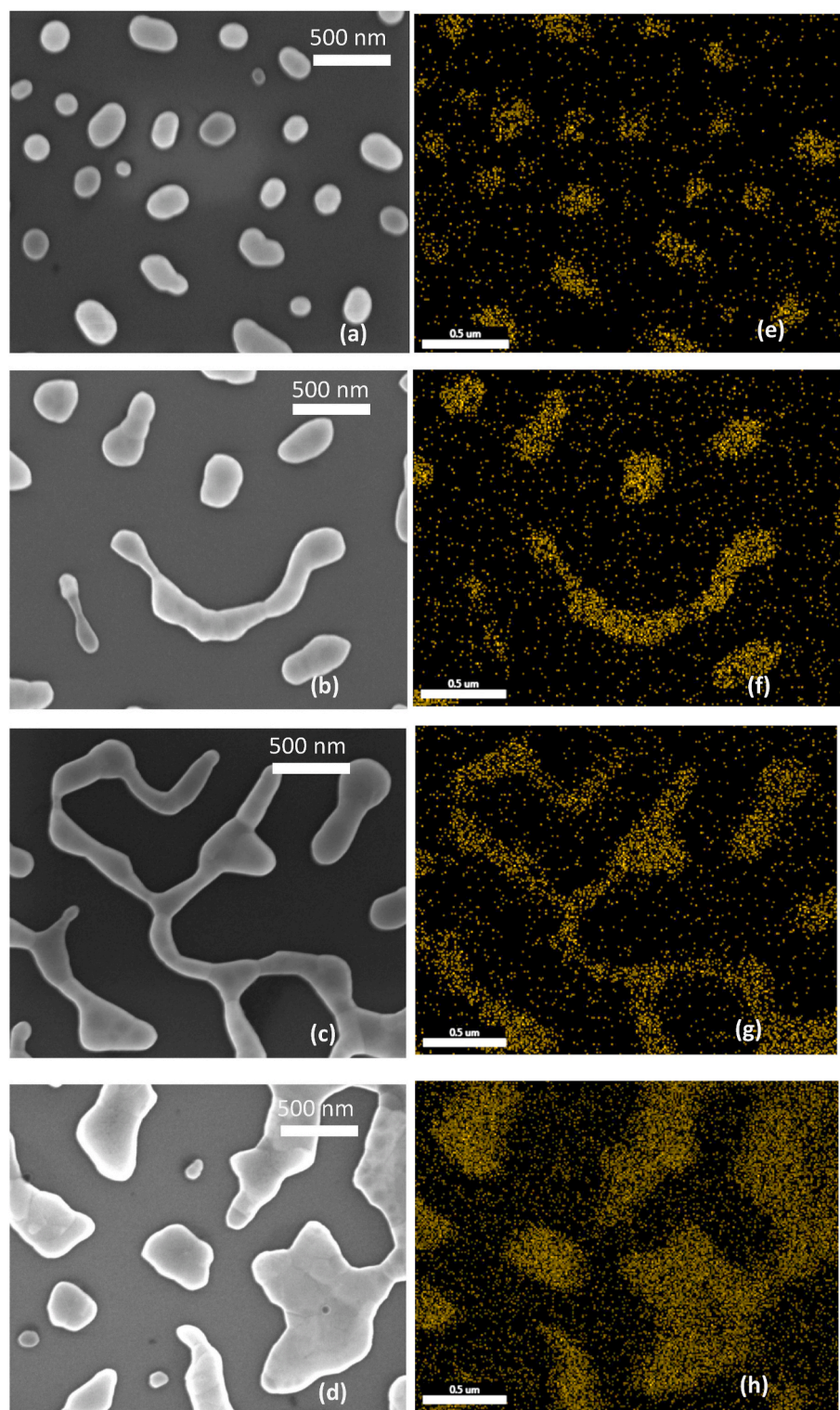


Fig. 3. SEM images of the samples prepared with sputtering of: a) 30 s; b) 40 s; c) 50 s; d) 60 s after annealing and the corresponding gold elemental mapping e) 30 s; f) 40 s; g) 50 s; h) 60 s.

enlightening the correlation between morphology of gold nanostructures and SERS in detail, our study also proposes an alternative, facile, scalable approach to fabricate SERS substrate based on gold nanostructures of high purity and excellent surface properties for analytical chemical applications.

4. Conclusion

Gold nanostructures of different morphologies were synthesized by heat treatment process of sputtered gold thin films. Shape and inter-spacing between neighbor nanostructures can be controlled conveniently by sputtering time. The results also showed that these parameters are critical to enhancement capability of the as-prepared gold

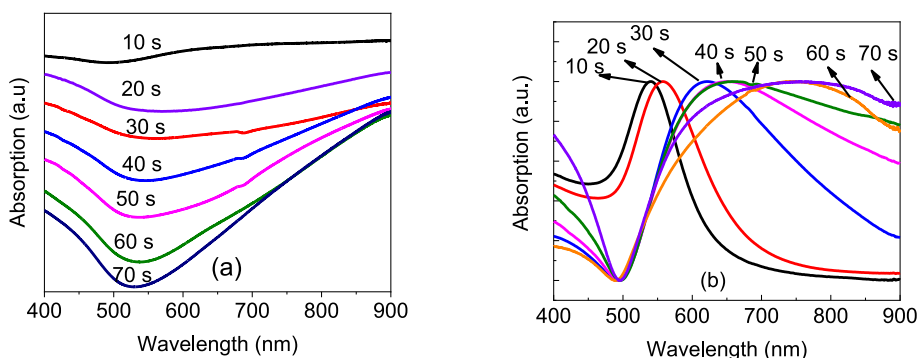


Fig. 4. (a) Absorption spectra of Au films with different sputtering time before annealing and (b) normalized absorption spectra of samples after heat treatment.

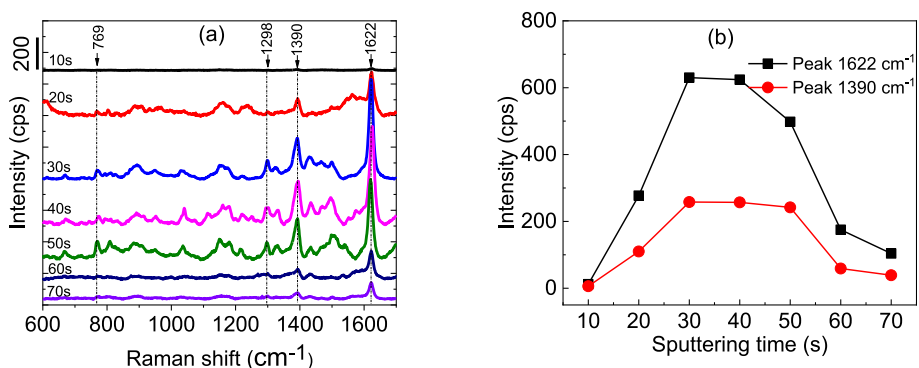


Fig. 5. (a) Raman spectra of MB (10^{-7} M) absorbed on gold nanoparticle arrays prepared with different sputtering times, (b) Dependence of Raman intensity of two main peaks at 1622 cm^{-1} and 1390 cm^{-1} on sputtering time.

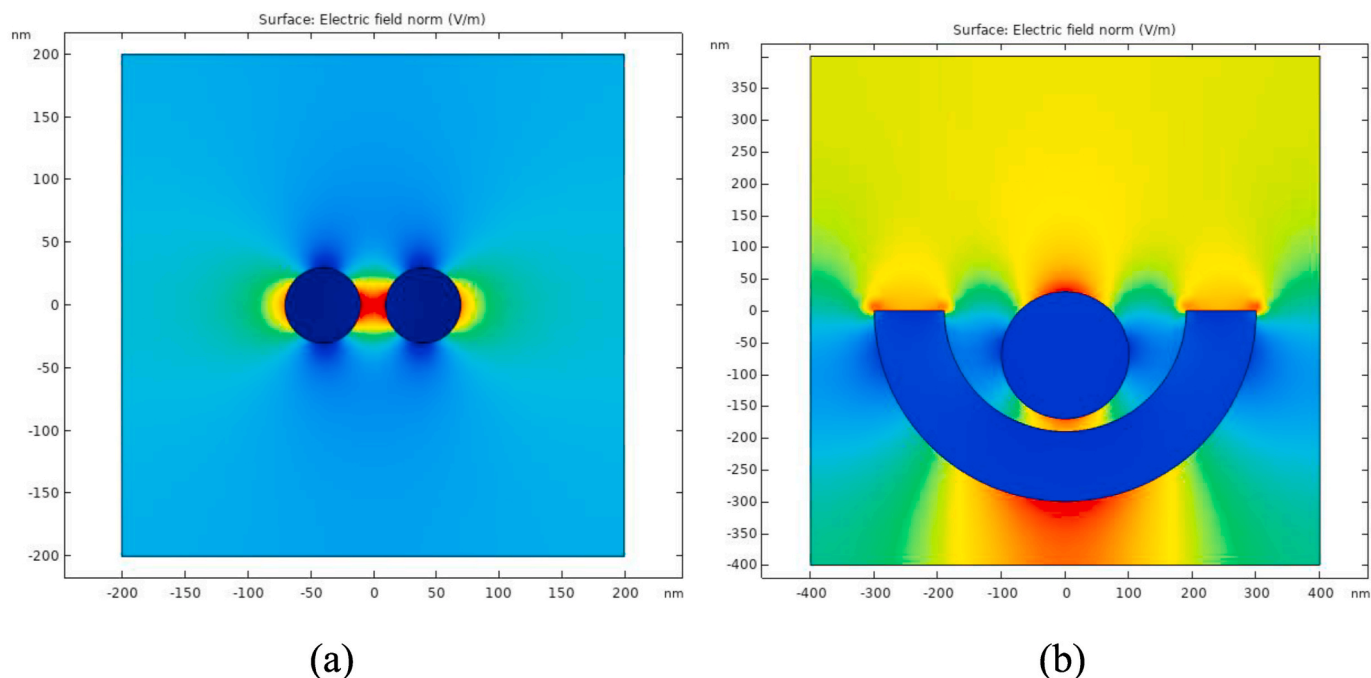


Fig. 6. Simulation of SERS effect of: (a) Au nanoparticles, (b) Au complex nanostructures.

nanostructure arrays. The gold nanostructures obtained with sputtering time of 40 s offer highest enhancement and allow detecting MB at low concentration of 10^{-10} M. The facile fabrication process and excellent surface properties thanks to the absence of any surfactants in the preparation make it an effective tool to trace substances at low concentration

for various practical applications.

Ethical statement

1) This material is the authors' own original work, which has not

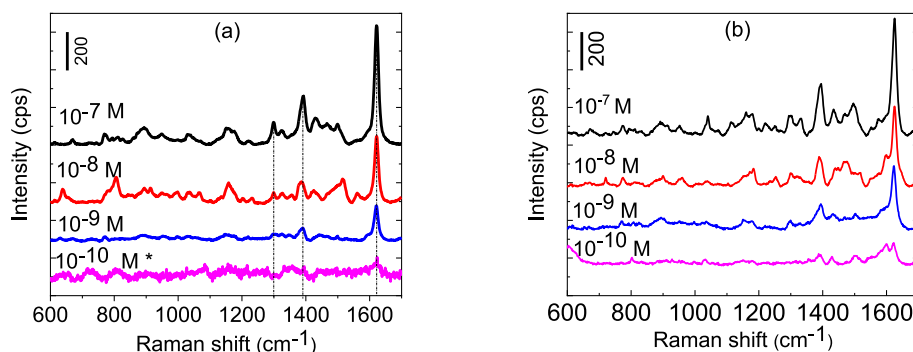


Fig. 7. Raman spectra of MB at various concentrations collected on Au nanoparticle array prepared with sputtering time of 30 s (a) and 40 s (b).

Table 1

Comparison of some nanomaterials used as SERS substrates.

Materials used	Synthesis method	Raman probe	Lowest concentration reported	References
MoS ₂ quantum dot/reduced graphene oxide	Solvothermal method	Methylene blue	10 ⁻⁸ M	[20]
Ag nanoparticles	Reduction silver salts	Rhodamine 6G	10 ⁻⁸ M	[22]
Ag; Ag/Cu thin films	Sputtering + annealing	Methylene blue	10 ⁻⁷ M	[23]
Ag loaded anodic Al ₂ O ₃	Anodization technique + Resistance heating vacuum evaporation	Rhodamine B	10 ⁻¹⁰ M	[24]
Ag/TiO ₂ nanotubes	Anodization + Resistance heating vacuum evaporation	Rhodamine B	10 ⁻⁵ M	[25]
ZnO/Au nanorods	Hydrothermal + sputtering	MB	10 ⁻⁹ M	[26]
CuO/Ag nanowires	Thermal oxidation + sputtering	MB	10 ⁻¹⁰ M	[27]
Au nanostructures	Sputtering + heat treatment	MB	10 ⁻¹⁰ M	This work

been previously published elsewhere.

2) The paper is not currently being considered for publication elsewhere.

3) The paper reflects the authors' own research and analysis in a truthful and complete manner.

4) The paper properly credits the meaningful contributions of co-authors and co-researchers.

5) The results are appropriately placed in the context of prior and existing research.

6) All sources used are properly disclosed (correct citation). Literally copying of text must be indicated as such by using quotation marks and giving proper reference.

7) All authors have been personally and actively involved in substantial work leading to the paper, and will take public responsibility for its content.

Data availability

The data that support the findings of this study are available from the corresponding author upon reasonable request.

CRediT authorship contribution statement

Thi Huyen Trang Nguyen: Investigation, Data curation, Writing – original draft. **Thi Mai Anh Nguyen:** Investigation. **Cong Doanh Sai:** Investigation. **Thi Hai Yen Le:** Investigation. **Thi Ngoc Anh Tran:** Investigation. **Thanh Cong Bach:** Investigation. **Van Vu Le:** Investigation. **Nguyen Hai Pham:** Investigation, Writing – review & editing. **An Bang Ngac:** Investigation, Writing – review & editing. **Viet Tuyen Nguyen:** Conceptualization, Investigation, Formal analysis, Supervision, Writing – review & editing. **Thi Ha Tran:** Conceptualization, Investigation, Supervision, Formal analysis, Methodology, Writing – original draft, Writing – review & editing, Funding acquisition, Project administration.

Declaration of competing interest

The authors declare that they have no known competing financial interests or personal relationships that could have appeared to influence the work reported in this paper.

Acknowledgement

This research is funded by Hanoi University of Mining and Geology, Vietnam, code T21-05. Ms. Thi Ha Tran was funded by Vingroup Joint Stock Company and supported by the Domestic Master/PhD Scholarship Programme of Vingroup Innovation Foundation (VINIF), Vingroup Big Data Institute (VINBIGDATA).

References

- [1] P.G. Yin, L. Jiang, T.T. You, W. Zhou, L. Li, L. Guo, S. Yang, Surface-enhanced Raman spectroscopy with self-assembled cobalt nanoparticle chains: comparison of theory and experiment, *Phys. Chem. Chem. Phys.* 12 (2010) 10781–10785, <https://doi.org/10.1039/c002662j>.
- [2] S. Dutta Roy, M. Ghosh, J. Chowdhury, S.D. Roy, J. Chowdhury, Adsorptive parameters and influence of hot geometries on the SER(S) S spectra of methylene blue molecules adsorbed on gold nanocolloidal particles, *J. Raman Spectrosc.* 46 (2015) 451–461, <https://doi.org/10.1002/jrs.4675>.
- [3] T. Yaseen, H. Pu, D.W. Sun, Functionalization techniques for improving SERS substrates and their applications in food safety evaluation: a review of recent research trends, *Trends Food Sci. Technol.* 72 (2018) 162–174, <https://doi.org/10.1016/j.tifs.2017.12.012>.
- [4] T.H. Tran, T.H.T. Nguyen, M.H. Nguyen, N.H. Pham, A.B. Ngac, H.H. Mai, V. T. Pham, T.B. Nguyen, K.H. Ho, T.T. Nguyen, V.T. Nguyen, Synthesis of ZnO/Au nanorods for self cleaning applications, *J. Nanosci. Nanotechnol.* 21 (2021) 2621–2625, <https://doi.org/10.1166/jnn.2021.19110>.
- [5] S. Ding, J. Yi, J. Li, B. Ren, R. Panneerselvam, Z. Tian, Nanostructure-based plasmon-enhanced Raman spectroscopy for surface analysis of materials, *Nat. Rev. Mater.* 1 (2016) 1–16, <https://doi.org/10.1038/natrevmats.2016.21>.
- [6] L.T.Q. Ngan, K.N. Minh, D.T. Cao, C.T. Anh, L. Van Vu, Synthesis of silver nanodendrites on silicon and its application for the trace detection of pyridaben pesticide using surface-enhanced Raman spectroscopy, *J. Electron. Mater.* 46 (2017) 3770–3775, <https://doi.org/10.1007/s11664-017-5284-4>.
- [7] W.R. Premasiri, J.C. Lee, A. Sauer-Budge, R. Théberge, C.E. Costello, L.D. Ziegler, The biochemical origins of the surface-enhanced Raman spectra of bacteria: a metabolomics profiling by SERS, *Anal. Bioanal. Chem.* 408 (2016) 4631–4647, <https://doi.org/10.1007/s00216-016-9540-x>.

- [8] S.M. Tabakman, Z. Chen, H.S. Casalongue, H. Wang, H. Dai, A new approach to solution-phase gold seeding for SERS substrates, *Small* 7 (2011) 499–505, <https://doi.org/10.1002/smll.201001836>.
- [9] L. Chen, H. Yan, X. Xue, D. Jiang, Y. Cai, D. Liang, Y.M. Jung, X.X. Han, B. Zhao, Surface-enhanced Raman scattering (SERS) active gold nanoparticles decorated on a porous polymer filter, *Appl. Spectrosc.* 71 (2017) 1543–1550, <https://doi.org/10.1177/0003702817703293>.
- [10] A. Ceja-Fdez, T. López-Luke, A. Torres-Castro, D.A. Wheeler, J.Z. Zhang, E. De La Rosa, Glucose detection using SERS with multi-branched gold nanostructures in aqueous medium, *RSC Adv.* 4 (2014) 59233–59241, <https://doi.org/10.1039/c4ra11055b>.
- [11] K. Lee, D. Yarbough, M.M. Kozman, T.J. Herrman, J. Park, Regulatory science sensitive SERS characterization and analysis of chlorpyrifos and aldicarb residues in animal feed using gold nanoparticles, *J. Regul. Sci.* 8 (2020) 1–14.
- [12] K. Kim, L.K. Kyung, H.B. Lee, S.S. Kuan, Surface-enhanced Raman scattering on aggregates of silver nanoparticles with, *J. Phys. Chem. C* 114 (2010) 18679–18685.
- [13] P. Mosier-Boss, Review of SERS substrates for chemical sensing, *Nanomaterials* 7 (2017) 142, <https://doi.org/10.3390/nano7060142>.
- [14] A. Vincenzo, P. Roberto, F. Marco, M.M. Onofrio, I. Maria Antonia, Surface plasmon resonance in gold nanoparticles: a review, *J. Phys. Condens. Matter* 29 (2017) 203002. <http://stacks.iop.org/0953-8984/29/i=20/a=203002>.
- [15] R.V. William, G.M. Das, V.R. Dantham, R. Laha, Enhancement of single molecule Raman scattering using sprouted potato shaped bimetallic nanoparticles, *Sci. Rep.* 9 (2019) 1–12, <https://doi.org/10.1038/s41598-019-47179-4>.
- [16] A.V.K.N.L. Dmitruk, Physical nature of anomalous optical transmission of thin absorptive corrugated films, *Pis'ma v ZhETF.* 65 (2010) 201–202.
- [17] A. Axlevitch, B. Gorenstein, G. Golan, Investigation of optical transmission in thin metal films, *Phys. Procedia.* 32 (2012) 1–13, <https://doi.org/10.1016/j.phpro.2012.03.510>.
- [18] J.H. Kim, P.J. Moyer, Thickness effects on the optical transmission characteristics of small hole arrays on thin gold films, *Opt Express* 14 (2006) 6595, <https://doi.org/10.1364/oe.14.006595>.
- [19] W. Rao, D. Wang, T. Kups, E. Baradács, B. Parditka, Z. Erdélyi, P. Schaaf, Nanoporous gold nanoparticles and Au/Al₂O₃ hybrid nanoparticles with large tunability of plasmonic properties, *ACS Appl. Mater. Interfaces* 9 (2017) 6273–6281, <https://doi.org/10.1021/acsami.6b13602>.
- [20] D. Wu, J. Chen, Y. Ruan, K. Sun, K. Zhang, W. Xie, F. Xie, X. Zhao, X. Wang, A novel sensitive and stable surface enhanced Raman scattering substrate based on a MoS₂ quantum dot/reduced graphene oxide hybrid system, *J. Mater. Chem. C.* 6 (2018) 12547–12554, <https://doi.org/10.1039/c8tc05151h>.
- [21] G.N. Xiao, S.Q. Man, Surface-enhanced Raman scattering of methylene blue adsorbed on cap-shaped silver nanoparticles, *Chem. Phys. Lett.* 447 (2007) 305–309, <https://doi.org/10.1016/j.cplett.2007.09.045>.
- [22] J.R. Ansari, N. Singh, R. Ahmad, D. Chattopadhyay, A. Datta, Controlling self-assembly of ultra-small silver nanoparticles: surface enhancement of Raman and fluorescent spectra, *Opt. Mater.* 94 (2019) 138–147, <https://doi.org/10.1016/j.optmat.2019.05.023>.
- [23] P. Nandhagopal, A.K. Pal, D. Bharathi Mohan, Fabrication of silver and silver-copper bimetal thin films using co-sputtering for SERS applications, *Opt. Mater.* 97 (2019) 109381, <https://doi.org/10.1016/j.optmat.2019.109381>.
- [24] X.G. Wang, J. Wang, J.F. Li, D.W. Tao, W.M. Zhou, Y. Li, C.W. Wang, Silver loaded anodic aluminum oxide defective photonic crystals and their application for surface enhanced Raman scattering, *Opt. Mater.* 105 (2020) 109982, <https://doi.org/10.1016/j.optmat.2020.109982>.
- [25] W.M. Zhou, J. Wang, X.G. Wang, J.F. Li, Y. Li, C.W. Wang, Ag loaded TiO₂ nanotube photonic crystals self-doped Ti³⁺ periodically by anodization process and their performance of surface enhanced Raman scattering, *Opt. Mater.* 99 (2020) 109567, <https://doi.org/10.1016/j.optmat.2019.109567>.
- [26] Q.K. Doan, M.H. Nguyen, C.D. Sai, V.T. Pham, H.H. Mai, N.H. Pham, T.C. Bach, V. T. Nguyen, T.T. Nguyen, K.H. Ho, T.H. Tran, Enhanced optical properties of ZnO nanorods decorated with gold nanoparticles for self cleaning surface enhanced Raman applications, *Appl. Surf. Sci.* (2019) 144593, <https://doi.org/10.1016/j.apsusc.2019.144593>.
- [27] T.H. Tran, M.H. Nguyen, T.H.T. Nguyen, V.P.T. Dao, Q.H. Nguyen, C.D. Sai, N. H. Pham, T.C. Bach, A.B. Ngac, T.T. Nguyen, K.H. Ho, H. Cheong, V.T. Nguyen, Facile fabrication of sensitive surface enhanced Raman scattering substrate based on CuO/Ag core/shell nanowires, *Appl. Surf. Sci.* 509 (2020) 145325, <https://doi.org/10.1016/j.apsusc.2020.145325>.